# Shared Admittance Control for Human-Robot Co-manipulation based on Operator Intention Estimation

Jonathan Cacace, Alberto Finzi and Vincenzo Lippiello
*PRISMA Lab, Dipartimento di Ingegneria Elettrica e Tecnologie dell'Informazione, Università degli Studi di Napoli, Federico II, via Claudio 21, 80125, Naples, Italy*

Keywords: Variable Admittance Control, Human-Robot Co-manipulation, Shared Control.

Abstract: Collaborative robots are increasingly employed in industrial workplaces, assisting human operators in decreasing the weight and the repetitiveness of their activities. In this paper, we assume the presence of an operator cooperating with a lightweight robotic arm, able to autonomously navigate its workspace, while the human co-worker physically interacts with it leading and influencing the execution of the shared task. In this scenario, we propose a human-robot co-manipulation method in which the autonomy of the robot is regulated according to the operator intentions. Specifically, the operator contact forces are assessed with respect to the autonomous motion of the robot inferring how the human motion commands diverges from the autonomous ones. This information is exploited by the system to adjust its role in the shared task, leading or following the operator and to proactively assist him during the co-manipulation. The proposed approach has been demonstrated in an industrial use case consisting of a human operator that interacts with a Kuka *LBR iiwa* arm to perform a cooperative manipulation task. The collected results demonstrate the effectiveness of the proposed approach.



## 1 INTRODUCTION

The widespread of lightweight robots enables to the development of novel service robotic applications, where humans and robots collaborate for the execution of shared tasks (Corrales et al., 2012). Such systems, also known as *cobots*, can share their workspace with human workers ensuring safe physical human-robot cooperation and allowing humans and robots to work side-by-side to merge their complementary abilities. In this perspective, advanced human-robot collaborative methods can facilitate the human work in all the operations difficult to automatize both in industrial tasks, such as assembly of heavy or complex parts (Giordano et al., 2008), and service tasks like cyclic object manipulation in dynamic environments.

This paper presents a framework that supports physical human-robot interaction during the execution of cooperative tasks. In the proposed approach, the robotic system on-line adapts its behaviour according to the operator intention, which is continuously estimated from his/her contact forces. In particular, we assume a shared control system, where the robot can autonomously execute a requested manipulation action, while the human operator can physically interact with the robot end effector, adjusting or modifying the motion of the robot or its target. In this scenario, human interventions can be associated with different intentions: lead the robot, slightly adjust its motion, change the target of the action, speed up its execution or use the manipulator as a passive tool. In order to exploit these interaction modes in an intuitive manner, human interventions are to be interpreted and the robotic behaviour must be consequently adapted.

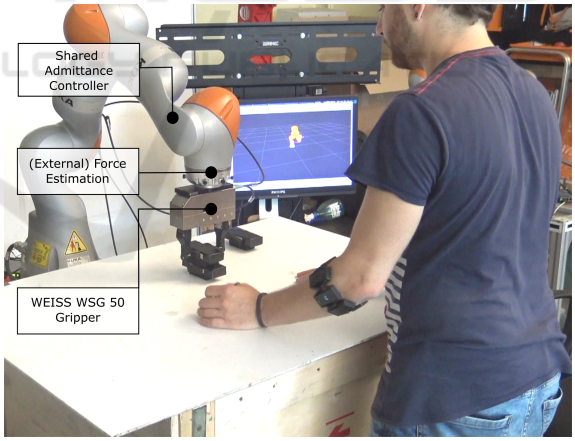


Figure 1: The human operator physically interacts with a lightweight manipulator during a cooperative manipulation task.



Cacace, J., Finzi, A. and Lippiello, V.
Shared Admittance Control for Human-Robot Co-manipulation based on Operator Intention Estimation.
DOI: 10.5220/0006831800610070
In *Proceedings of the 15th International Conference on Informatics in Control, Automation and Robotics (ICINCO 2018) - Volume 2*, pages 61-70
ISBN: 978-989-758-321-6

For this purpose, we propose a shared control system supporting different autonomous and semi-autonomous operative modes, regulated according to the operator intentions, which are interpreted considering contact forces provided by the human operator. In this context, the contact forces are continuously assessed to inform the robot about the next target point to reach or to interpret the motion deviation intended by the human during cooperative manipulation. The intention recognition process relies on a *3-Layer Neural Networks* that, upon receiving as input the robot motion direction and the operator contact forces, infers the intention of the operator to follow/contrast the manipulator motion towards a target point, deviate from the latter, or use the robot manipulator in direct manual control in order to perform other actions. In this scenario, the robot can operate in either a passive or an active mode. When the estimated intention of the human is not aligned with the target of the robot, the latter passively follows the human guidance and the robot behaviour is fully compliant to the operator contact. On the other hand, when human interventions are coherent with respect to the current robot target, the robotic system can keep executing the current task, while suitably adjusting its motion trajectory following the corrections provided by the operator. In summary, this work proposes a novel mixed-initiative co-manipulation framework in which physical interaction, interpretation of the human interventions, task/target switching, and admittance adjustment are seamlessly integrated. The aim is to conciliate, in a flexible and adaptive manner, the precision and the strength of the robotic system with the dexterity and the decisional capability of the human operators.

In order to demonstrate the proposed framework, we designed a human-robot interaction setup (see Fig. 1), where the human operator cooperates with a Kuka *LBR iiwa* robot during the execution of a manipulation task. In this scenario, the effectiveness of the system is assessed by comparing the fatigue and the effort needed by the operator to accomplish the task with and without the assistance of the proposed framework.

The remainder of this paper is organized as follows. In Section 2 a brief overview of related works is presented, in Section 3 the system architecture is described, while in Sections 4 and 6 the human intention estimation process is discussed. Section 5 describes how the operator intention estimation is exploited in the shared controller. Finally, in Section 7 an experimental case study to test the effectiveness of our approach is presented.

## 2 RELATED WORKS

Estimating the operator intentions in order to regulate the robot behavior during the execution of a shared task is crucial in any kind of Human-Robot collaboration activity (Hoffman and Breazeal, 2004; Hoffman and Breazeal, 2007). Flexible and natural interaction with humans is often needed to enable cooperation with robots in social and industrial or service robotic applications. This problem has been addressed by different works in the robotic literature. For instance, a method to adapt the role of the robot considering operator fatigue during a co-manipulation task is presented in (Peternel et al., 2016), in which the robot learns by imitation how to assist the operator taking contact forces into account, but without inferring his/her intentions. More related to our work, in (Jlassi et al., 2014) a shared trajectory generator based on operator force contact is proposed to translate human intentions into ideal trajectories the robot should follow. In this case an on-line trajectory generator is combined with a classical impedance control system, instead we rely on an integrated intention estimation system. Other approaches exploit human intention estimation to increase the efficiency of task planning algorithms ((Hoang and Low, 2013) and (Caccavale et al., 2016)). Intention recognition methods typically consider external forces excreted by the human operator on the robot side to regulate the low level behaviour of the robot (Park et al., 2016)(Peternel and Babic, 2013)(Gribovskaya et al., 2011)(Li et al., 2015). Differently, our approach is aimed to adapt robot task execution, without influencing the low level control of the robot.

In (Li and Ge, 2014) motion intention of the human partner is detected using the human limb model to estimate the desired trajectory, while in (Kouris et al., 2017) external force information is exploited to discern between a human contact and an unexpected collision. Human motion estimation is also deployed in (Ge et al., 2011), where the authors exploit Neural Networks to extract human motion parameter and predict whether the human interventions are active or passive. In contrast, we exploit Neural Networks to directly classify the human force contacts with respect to the robot motion during the execution of a cooperative task, as already proposed in (Cacace et al., 2018).

Several other works exploit visual sensors to predict human intentions, as in (Bascetta et al., 2011), where human motion trajectories are monitored to predict the human presence in robotic cells, or like in (Cacace et al., 2016), where the authors address the problem of implicitly selecting a robot of a team given the sequence of commands issued by the op-

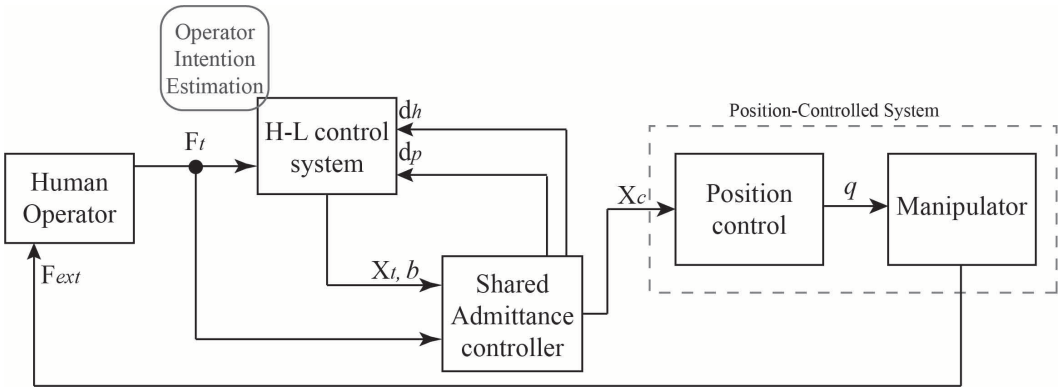


Figure 2: Shared control architecture.

erator. Other approaches propose probabilistic methods to infer human intentions. For instance, in (Kelley et al., 2008) a Hidden Markov Model (*HMM*) has been used to estimate the most likely human activity perceived by a mobile robot, or in (Awais and Henrich, 2010) and (Best and Fitch, 2015), where Bayesian inference and weighted probabilistic state machines, respectively, have been used to perform intention recognition.

Notice that, in contrast with other approaches to physical human-robot interaction framework based on human intention estimation that asses operator intentions to enable a compliant physical human-robot interaction, we use this information to switch from an active to passive participation of the robot to the shared task and replan when a novel intended target is estimated from the human physical interventions. In this perspective, the approach proposed in this work can be related to the one proposed by (Cacace et al., 2014) for shared teleoperation of an aerial vehicles; however this approach is less explored in physical collaborative manipulation.

## 3 CONTROL ARCHITECTURE

In this section, we describe the proposed control architecture, which is depicted in Figure 2. The motion of the robot is managed by the *Shared Admittance Controller* module, whose goal is to command the robot to reach desired targets. As for the robotic manipulator, we assume to control the position and orientation of its end effector, relying on the robot inner control loop to solve inverse kinematic problem; we also assume that the (external) forces acting on the gripper are directly estimated by the robot itself. During physical human-robot interaction, the operator contact forces exerted on the end effector are continuously monitored by the *H-L control system* that exploits the *Operator Intention Estimation* sub-module to assess human intentions. This information is exploited by the *Shared Admittance Controller* module in order to suitably adapt the robot behaviour during the execution of the cooperative task. In the following, all modules of the architecture are further detailed.

As already stated, the *Human Operator* can physically interact with the manipulator moving its end effector within a defined workspace. In particular, we assume that he/she applies a force $F_t$ on the robot end effector and perceives a force feedback $F_{ext}$. On the other hand, the *H-L control system* is responsible to select the target point to be reached in order to accomplish a given task. The target point $X_t$ is sent to the *Shared Admittance Controller* along with the classified user behaviour $b$ to start the motion of the robot. This module is to generate the motion data $X_d$ needed to reach the target $X_t$. In addition, exploiting an admittance controller, this module is responsible to combine the autonomous motion data with the control inputs $F_t$ provided by the operator. In physical Human-Robot Interaction, the admittance control is used to establish a dynamic relationship between the forces applied to the robot and the displacement from its desired position (Hogan, 1984). The admittance controller is described by the typical second-order relationship:

$$m\ddot{x} + d\dot{x} + kx = F \quad (1)$$

that can be represented as (see (Siciliano and Villani, 2000)):

$$M_d(\ddot{X}_c - \ddot{X}_d) + D_d(\dot{X}_c - \dot{X}_d) + K_d(X_c - X_d) = F_t \quad (2)$$

Where $M_d$, $D_d$ and $K_d$ are the desired virtual inertia, the virtual damping and the virtual stiffness, respectively, modelling the behaviour of the system as a mass-spring-damper system. Typically, during co-manipulation tasks the operator aims at moving the robotic arm in free motion. For this reason, the stiffness $K_d$ is set to zero in order to nullify the elastic

behaviour of the system. The output of this module is the compliant position $X_c$, representing the control command for the *Position-Controlled System*. Finally, the commanded position is converted into joint values $q$, which are then applied to the manipulator. When no target is selected by the *H-L control system*, the position $X_t$ is set to the current position of the end effector.

The *Operator Intention Estimation* sub-module is used to asses the operator intentions. Its goal is to estimate human intentions of following or diverging from the autonomous motion, while classifying different possible behaviours of the user. The operator intentions are inferred exploiting a Neural Network (see Section 4) using the following information: the contact forces $F_t$ the operator exerts on the robotic gripper, the motion direction $d_h$ inducted by the operator, and the motion direction $d_p$ generated by the shared controller. The classified behaviour is then sent to the *Shared Controller* module that uses this information to modify its level of autonomy during the execution of the task as described in Section 5. In order to lead the robot towards a new position, the *H-L control system* must select the target the operator is trying to reach. For this reason, we assume that, for each task, the system is provided with the set of possible positions to be reached during the execution of that task. This module exploits this knowledge to infer the operator intention to move the manipulator toward one of these points.

# 4 OPERATOR INTENTION ESTIMATION

In this section, we detail the operator intention estimation process. As already stated, this process relies on a *Neural Network* classifier (Bishop, 1995) properly adapted to our domain. An Artificial Neural Network (*ANN*) is composed by a list of nodes, called *artificial neurons* distributed on multiple layers. Typically, data to classify travel from the first (*input*) to the last (*output*) layer, possibly after traversing different internal (*hidden*) layers. In this structure, the number of nodes of the first and last layer, represents the number of expected input parameters and the number of possible output classes, respectively. In order to classify human intentions, we designed a neural network of three layers. The input and output layers contain, respectively, 3 and 4 nodes, while we considered 25 nodes in the middle hidden layer. Our aim is to use this neural network to compare the motion direction intended by the operator with respect to the one planned and executed by the autonomous system in order to understand whether the human and the robot activities and goals are aligned or not. The input of this network is calculated starting from the information about the contact forces $F_t$, the motion direction induced by the operator $d_c$, the motion generated by the controller $d_d$ to follow the path toward the target point. We assume that only linear segments are used to navigate the workspace. In addition, the closest point $C_p$ of the end effector with respect to the path segment under execution is continuously calculated in order to inform the system on how far is the robot with respect to the planned trajectory. Therefore, the input of the Neural Network is represented by:

- $||F_t||$: The magnitude of forces exerted by the operator.
- $||X_c - C_p||$: The distance between the current end effector position and the closest point on the path segment under execution.
- $\angle(\overrightarrow{d_c}, \overrightarrow{d_d})$: The deviation between the planned and human motions, calculated as the angle between the two movement vectors.

Table 1: Operator behaviour interpretation.

| *Class ID* | *Class Name* | *Description* |
|---|---|---|
| *#0* | *Accompany* | The operator is touching the end effector without providing any contribution to the task. |
| *#1* | *Opposite* | The operator moves the manipulator in the opposite direction of the planned path. |
| *#2* | *Coinciding* | The operator moves the manipulator following the planned path. |
| *#3* | *Coinciding deviation* | The operator deviates from the planned path, trying to reach a target. |

Table 1 reports the classes recognized by the Neural Network along with a brief description of the associated interpretation of the operator behaviours. We distinguish the following four behaviours (three of them are shown in Figure 3). In the first place, we consider the case in which the operator is in physical contact with the gripper, but only accompanying the manipulator (*i.e.* waiting that the autonomous system accomplishes its goal), without providing any additional contribution to the task execution (*Accompany*). The second case is illustrated in Figures 3(c) and 3(d), where the operator is driving the robot in the opposite direction with respect to the trajectory and target planned by the autonomous system (*Opposite*). Instead, in Figure 3(a), the operator is moving the robot end effector in the same direction of the planned path

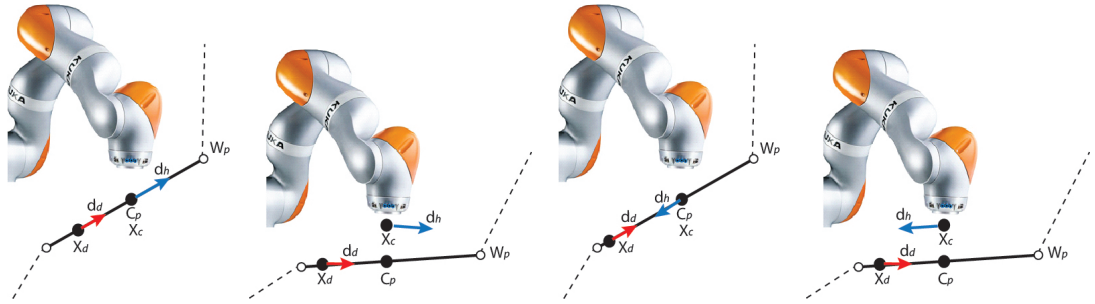


(a) Coinciding behaviour (b) Coinciding deviation behaviour (c) Opposite behaviour (d) Opposite behaviour

Figure 3: Different operator behaviours. The red arrow represents the autonomous motion direction $D_d$, the blue arrow is the operator motion direction $d_h$. The robot is moving toward the waypoint $W_p$, while $C_p$ is the closest point between the end effector and the planned path.

Table 2: Confusion Matrix.

| | *0* | *1* | *2* | *3* |
|---|---|---|---|---|
| *0* | 89.2% | 0.23% | 10.57% | 0% |
| *1* | 3.2% | 95.02% | 0.0% | 1.78% |
| *2* | 6.3% | 0.6% | 84.1% | 9.0% |
| *3* | 0.0% | 5.58% | 5.12% | 89.3% |

(*Coinciding*). Finally, Figure 3(b) illustrates the case in which the operator moves the end effector away from the planned path, but he/she is still trying to reach the planned target (*Coinciding deviation*).

As for the training of the Neural Network, we involved a group of 10 users (students and researchers) asking them to physically interact with the robotic arm (10 minutes each) in different interactive supervised situations covering the *intentions classes* introduced above. During the training phase, the manipulator is programmed to move towards predefined waypoints. This way, we collected several examples of the operator interactive behaviour for each class. The final training set used for the system evaluation is composed of about 10000 samples and the network has been trained using the back propagation function. Once trained, we tested the recognition system with a different group of users similarly composed, interacting with the manipulator whose task is to follow a preplanned squared path with its end effector. Table 2 reports the *confusion matrix* of the intention classifier showing that the recognition system has been able to correctly classify 89.4% of the samples.

# 5 SHARED ADMITTANCE CONTROL BASED ON OPERATOR INTENTION ESTIMATION

In this section, we discuss how the robot uses the estimation of the operator intentions to adapt its role and interaction mode during the execution of the shared task. As already stated, the robot can switch from a *passive* to an *active* operative mode. In the first case, the manipulator is fully compliant to operator contact without providing any contribution to the task, while in the second case the manipulator is actuated to better assist the operator in reaching the target position $X_{wp} = (x_{wp}, y_{wp}, z_{wp})$. Referring to schema depicted in Figure 2, in order to reach the target state, a velocity reference $\dot{X}_d$ command at a certain time $i$ is generated as follow:

$$\ddot{X}_{d_i} = \omega^2 e_p - 2\zeta \dot{X}_{d_{i-1}} \tag{3}$$

$$\dot{X}_{d_i} = \dot{X}_{d_{i-1}} + \ddot{X}_{d_i}\tau \tag{4}$$

Where $\omega$ and $\zeta$ are gains representing frequency and damping of the system respectively, while $\tau$ is the sampling time of the controller. The position error $e_p = (X_t - X_c)$ is calculated as the distance of the manipulator $(X_c)$ from the designed target position $(X_t)$. The velocity obtained with the Formula 4 is successively integrated to get the desired position of the robot:

$$X_{d_i} = X_{d_{i-1}} + \dot{X}_{d_i}\tau \tag{5}$$

The compliant behaviour of the manipulator is enabled with the following formula, in which the compliant position of the end effector is calculated considering both the operator forces and the autonomous control data:

$$\ddot{X}_{c_{i+1}} = \frac{M\ddot{X}_{d_i} + D(\dot{X}_{d_i} - \dot{X}_{c_i}) + F_t}{M} \tag{6}$$

We allow the switching from the passive to the active mode by nullifying the autonomous contribution of the robot from the previous equation, i.e. by setting to zero the desired acceleration and velocity, as described in Algorithm 1. In particular, we want to inhibit the contribution of the autonomous motion when the user behaviour is recognized as *Opposite*, for this purpose we set $\ddot{X}_{d_i} = \dot{X}_{d_i} = 0$ in Equation 6. This way, the robot is fully compliant to human contact forces, without trying to came back to the initial position $X_{d_i}$. Differently, when the operator behaviour is classified as *Coinciding* or *Coinciding deviation* we have two different situations associated with two different target points selected by the *H-L control system*. In the *Coinciding* case, the point to reach is represented by the one assessed as the current operator target $X_{wp}$. Instead, in the second case, a new target point is selected in order to help the operator in order to move back the end effector towards to the planned path. Specifically, in order to provide the human with a smooth guidance towards the planned path, during *Coinciding deviation*, the robotic system is provided with a target point $X_{cp}$, which is a midpoint between the final target position $X_t$ and the closest point to the planned path $C_p$. This target point is then continuously updated during the *Coinciding deviation* until a different human intention is recognized. Notice that, the described approach to *Coinciding deviation* not only provides the operator with a smooth guidance toward the planned path and the target point, but also produces a force feedback on the human side, which is associated with a feeling of the displacement between the current robot position and the planned path. This haptic feedback is conceptually similar to the one already proposed by (Cacace et al., 2014) for mixed-initiative teleoperation of aerial vehicles.

Finally, in order to avoid discontinuity of the control input that could induce instability in the system, a smooth transition between the different levels of autonomy (e.g from passive to active and viceversa or from coinciding to deviating and viceversa) has to be considered. For this reason we adopted a time-vanishing *smoothing term* as proposed by (Lippiello et al., 2016). Specifically, given a switch from the active to the passive control mode which starts at time $t = 0$, the velocity command introduced in Equation 7 is computed as follow:

$$v(t) = v_a(t) + e^{1/\gamma}(v_p(0) - v_a(0)) \tag{7}$$

where $\gamma$ is a time constant representing the duration of the transition phase, while $v_a$ and $v_p$ are the velocity commands related to the system acting in the active and passive mode, respectively.

Algorithm 1: Shared admittance control based on operator intention.

**Require:** Target point: $X_{wp}$, Behaviour: $b$
**procedure** $X_c$ = $shared\_controller(X_{wp}, b)$
  **while** $X_{wp}$ is not reached **do**
    **if** $b$ == *Opposite* **then**
      $\ddot{X}_d = 0.0$
      $\dot{X}_d = 0.0$
    **else**
      $e_p = (X_t - X_c)$
      $\ddot{X}_{d_i} = \omega^2 e_p - 2\zeta\dot{X}_{d_{i-1}}$
      $\dot{X}_{d_i} = \dot{X}_{d_{i-1}} + \ddot{X}_{d_i}\tau$
      **if** $b$ == *Coinciding_deviation* **then**
        $X_t = X_{cp}$
      **else**
        $X_t = X_{wp}$
      **end if**
    **end if**
  **end while**
**end procedure**

# 6 PREDICTION OF THE OPERATOR TARGET

In the proposed system, the operator intention estimation is also exploited to recognize his/her intention to bring the robot towards specific target positions within the workspace. In particular, we assume that each task is associated with a set of possible states characterized by target positions to be reached in order to accomplish a given task. We also assume that this set is available to the system and can analysed by the *H-L control system* module in order to assess the most probable target point the operator is trying to reach. For this purpose, the system generates a set of virtual trajectories, each connecting the current position of the end effector with an available target point. The operator intention is estimated with respect to all the virtual trajectories, until the estimated intention becomes *Coinciding* for only one trajectory; this trajectory is then assumed as the one aimed by the operator. This decision process is exemplified in Figure 4, where the system is initialized with four states. At the start, the operator is not providing any contribution to the task, hence the system cannot infer the target (in Figure 4(a) all the virtual trajectories are colored in black). Successively, the operator starts moving the end effector toward one of the target points, while the system identifies two of them as target candidates (in Figure 4(b) the two red paths represent the target candidates). Finally, the operator intention becomes *Coinciding* for only one trajectory, hence the associated

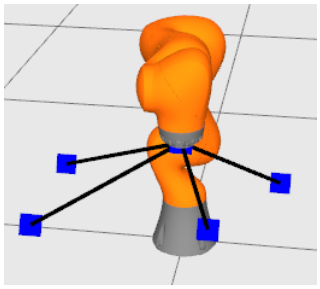

(a) No target candidates

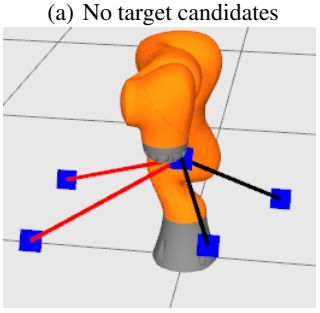

(b) Two target candidates

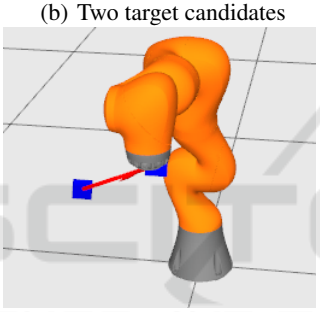

(c) Target predicted

Figure 4: Prediction of the operator target.

state is selected as the one intended by operator and a cartesian trajectory is generated and executed (Figure 4(c)). On the other hand, if the operator intention is classified as *Opposite* during the execution of the selected trajectory, we assume that the operator target may be changed/refined hence a novel target decision process starts in order to generate the new target along with the new trajectory.

Table 3: Experimental Results.

| | *min.* | *max.* | *mean* | *std.* |
|---|---|---|---|---|
| Fatigue *(S)* | 1.9 | 143.3 | 24.5 | 17.26 |
| Fatigue *(P)* | 1.8 | 202.7 | 45.3 | 30.4 |
| Force *(S)* | 0 | 32.04 | 9.14 | 8.31 |
| Force *(P)* | 0 | 57 | 16.59 | 13.9 |

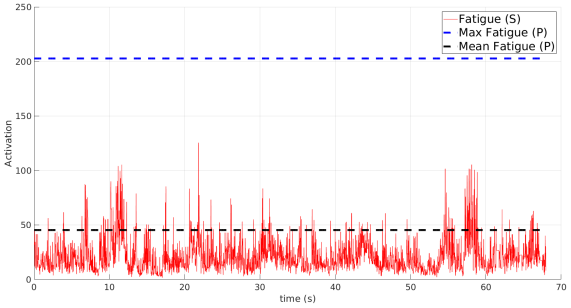


(a) Operator fatigue in shared operative mode, compared with the maximum and mean fatigue values in passive mode.

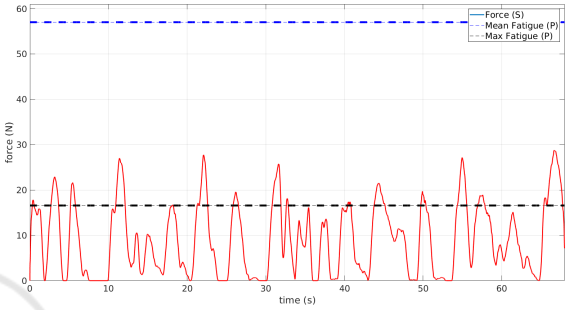


(b) Operator contact force in shared operative mode, compared with the maximum and mean contact force values in passive mode.

Figure 5: Operator fatigue (a) and contact force (a).

## 7 CASE STUDY

The effectiveness of the proposed system has been assessed by defining a collaborative manipulation case study where a human worker cooperates with a lightweight robotic arm in order to grasp different objects and plug them in predefined locations. In order to show the advantage of the presented approach, a user already trained on the system performed repetitive tries of the designed task. We compared the system performance with respect to a baseline version of the framework in which the *H-L control system* is disabled and the manipulator operates as a completely passive robotic assistant. We refer to this operative mode as *Passive* (*P*). During test execution, we evaluated both task performance, considering the distance covered by the manipulator, and the human physical effort, measuring operator muscle *fatigue* and the norm of the force that he/she exerts on the manipulator. In this context, we measured muscle fatigue exploiting a set of electromyographic sensors, that provide us the activation level of the arm muscles. The experimental setup is depicted in Figure 6. Tests have been performed using the Kuka *LWR iiwa* robot, controlled via *ROS* middleware running on GNU/Linux OS, as in (Hennersperger et al., 2016). Regarding the

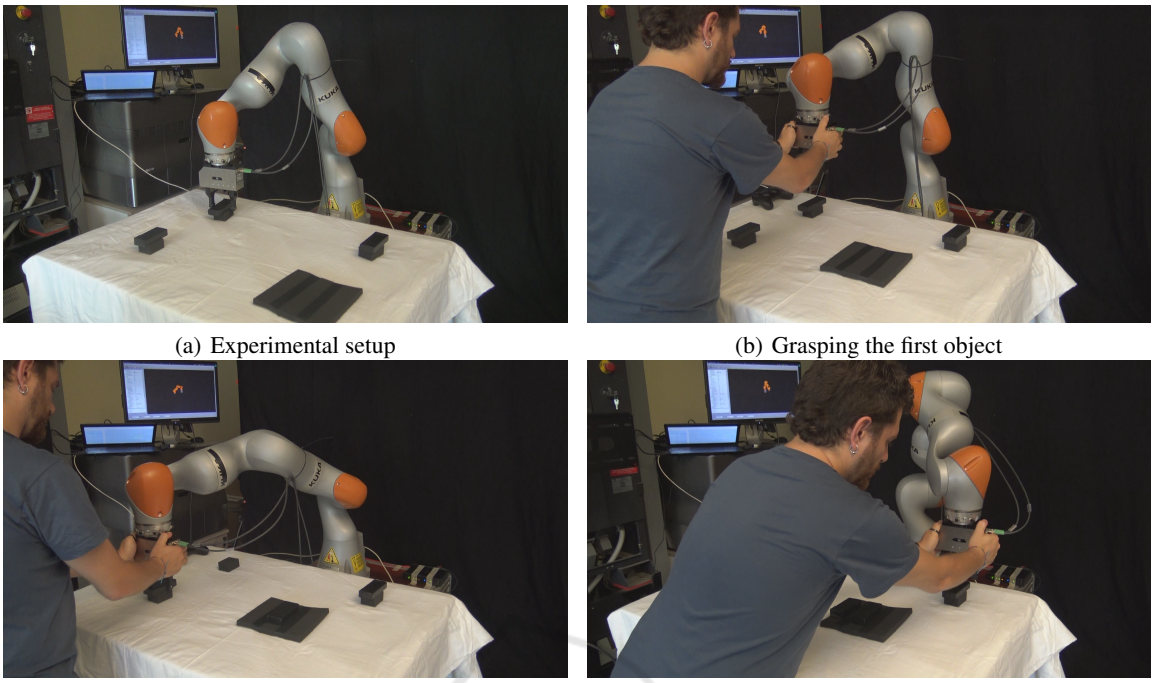

(a) Experimental setup (b) Grasping the first object

(c) Grasping the second object (d) Grasping the last object

Figure 6: Human operator interacting with the Kuka iiwa equipped with WEISS Wsg50 during system testing.

gripper, we used the *WEISS Wsg50* controlled via a standard joypad to close and open its fingers. The overall manipulation task consists in grasping three objects, one at a time, bringing them to specific positions of the workspace, as shown in Figures 6(b) - 6(d). Therefore, task accomplishment requires six actions: three picks and three places. During the experiment, the operator is free to decide when to interact with the manipulator by selecting any of the available objects and positions as targets. A demonstrative video is available at this link: goo.gl/7xLA4r. Table 3 reports the mean of norm of human force and fatigue data over all the the experiments. In this table, the minimum, the maximum, the mean, and the standard deviation of the operator fatigue and the norm of the force related to shared (*S*) and passive (*P*) settings are reported. As for task performance, the mean distance covered by the manipulator end effector during the tests is 3.6 meters in the shared setting against the 4.51 meters in the passive mode, therefore the shared system not only enables a more comfortable interaction, but also a more efficient task execution.

The benefits of the proposed system are also illustrated in Figure 5, where we compare the human force and fatigue measured in the two settings during one of the experiments. For this purpose, illustrate the EMG signal (red plot in Figure 5(a)) and the force contact one (red plot in Figure 5(b)) detected in the shared mode (adaptive shared controller), with respect to the maximum and mean values (upper and lower dotted lines in Figure 5) of the same signals obtained in the passive mode. The clear reduction of both fatigue and force highlight the advantage of the approach.

## 8 CONCLUSION

We presented a framework that supports physical human-robot interaction in collaborative manipulation tasks. In the proposed approach, the human physical interaction with the robotic system is continuously assessed in order to infer the operator intentions with respect to the current robotic behavior. The recognized intentions are then exploited by the shared control system to on-line adjust the robotic behavior with respect to the human interventions. We described the overall architecture detailing the operator intention estimation method and the associated shared control system. The proposed system has been demonstrated presenting the case study of a collaborative manipulation tasks, where the performance of the proposed method have been compared with respect to a baseline system relying on an admittance controller with disabled intention estimation and the associated adaptive mechanisms. The collected results shows the effectiveness of the approach in terms of both task performance and human fatigue.

## ACKNOWLEDGEMENTS

The research leading to these results has been supported by the ERC AdG-320992 RoDyMan, H2020-ICT-731590 REFILLs and MADWALK projects respectively. The authors are solely responsible for its content. It does not represent the opinion of the European Community and the Community is not responsible for any use that might be made of the information contained therein.

## REFERENCES

Awais, M. and Henrich, D. (2010). Human-robot collaboration by intention recognition using probabilistic state machines. In *19th International Workshop on Robotics in Alpe-Adria-Danube Region (RAAD 2010)*, pages 75–80.

Bascetta, L., Ferretti, G., Rocco, P., Ardö, H., Bruyninckx, H., Demeester, E., and Lello, E. D. (2011). Towards safe human-robot interaction in robotic cells: An approach based on visual tracking and intention estimation. In *2011 IEEE/RSJ International Conference on Intelligent Robots and Systems*, pages 2971–2978.

Best, G. and Fitch, R. (2015). Bayesian intention inference for trajectory prediction with an unknown goal destination. In *2015 IEEE/RSJ International Conference on Intelligent Robots and Systems (IROS)*, pages 5817–5823.

Bishop, C. M. (1995). *Neural Networks for Pattern Recognition*. Oxford University Press, Inc., New York, NY, USA.

Cacace, J., Finzi, A., and Lippiello, V. (2014). A mixed-initiative control system for an Aerial Service Vehicle supported by force feedback. In *IEEE International Conference on Intelligent Robots and Systems*.

Cacace, J., Finzi, A., and Lippiello, V. (2016). Implicit robot selection for human multi-robot interaction in Search and Rescue missions. In *25th IEEE International Symposium on Robot and Human Interactive Communication, RO-MAN 2016*.

Cacace, J., Finzi, A., and Lippiello, V. (2018). Enhancing human-robot collaborative task execution via contact force classification. *Human Friendly Robotics*.

Caccavale, R., Cacace, J., Fiore, M., Alami, R., and Finzi, A. (2016). Attentional supervision of human-robot collaborative plans. In *25th IEEE International Symposium on Robot and Human Interactive Communication, RO-MAN 2016*.

Corrales, J. A., Garcia Gomez, G. J., Torres, F., and Perdereau, V. (2012). Cooperative tasks between humans and robots in industrial environments. *International Journal of Advanced Robotic Systems*, 9.

Ge, S. S., Li, Y., and He, H. (2011). Neural-network-based human intention estimation for physical human-robot interaction. In *2011 8th International Conference on Ubiquitous Robots and Ambient Intelligence (URAI)*, pages 390–395.

Giordano, P. R., Stemmer, A., and Arbter, K. (2008). Robotic Assembly of Complex Planar Parts : An Experimental Evaluation. pages 22–26.

Gribovskaya, E., Kheddar, A., and Billard, A. (2011). Motion learning and adaptive impedance for robot control during physical interaction with humans. In *2011 IEEE International Conference on Robotics and Automation*, pages 4326–4332.

Hennersperger, C., Fuerst, B., Virga, S., Zettinig, O., Frisch, B., Neff, T., and Navab, N. (2016). Towards mri-based autonomous robotic us acquisitions: A first feasibility study. *IEEE transactions on medical imaging*.

Hoang, T. N. and Low, K. H. (2013). Interactive POMDP lite: Towards practical planning to predict and exploit intentions for interacting with self-interested agents. *CoRR*, abs/1304.5159.

Hoffman, G. and Breazeal, C. (2004). Collaboration in human-robot teams. *Proceeding of the AIAA 1st Intelligent Systems Technical Conference*, page 1.

Hoffman, G. and Breazeal, C. (2007). Effects of anticipatory action on human-robot teamwork efficiency, fluency, and perception of team. *Proceeding of the ACM/IEEE international conference on Human-robot interaction - HRI '07*, page 1.

Hogan, N. (1984). Impedance Control: An Approach to Manipulation. *IEEE American Control Conference*, pages 304–313.

Jlassi, S., Tliba, S., and Chitour, Y. (2014). An Online Trajectory generator-Based Impedance control for co-manipulation tasks. *IEEE Haptics Symposium, HAPTICS*, pages 391–396.

Kelley, R., Nicolescu, M., Tavakkoli, A., Nicolescu, M., King, C., and Bebis, G. (2008). Understanding human intentions via hidden markov models in autonomous mobile robots. In *2008 3rd ACM/IEEE International Conference on Human-Robot Interaction (HRI)*, pages 367–374.

Kouris, A., Dimeas, F., and Aspragathos, N. (2017). Contact distinction in human-robot cooperation with admittance control. *2016 IEEE International Conference on Systems, Man, and Cybernetics, SMC 2016 - Conference Proceedings*, pages 1951–1956.

Li, Y. and Ge, S. S. (2014). Human–Robot Collaboration Based on Motion Intention Estimation. *IEEE/ASME Transactions on Mechatronics*, 19(3):1007–1014.

Li, Y., Tee, K. P., Chan, W. L., Yan, R., Chua, Y., and Limbu, D. K. (2015). Continuous Role Adaptation for Human Robot Shared Control. *IEEE Transactions on Robotics*, 31(3):672–681.

Lippiello, V., Cacace, J., Santamaria-Navarro, A., Andrade-Cetto, J., Trujillo, M. ö., Esteves, Y. R., and Viguria, A. (2016). Hybrid visual servoing with hierarchical task composition for aerial manipulation. *IEEE Robotics and Automation Letters*, 1(1):259–266.

Park, J. S., Park, C., and Manocha, D. (2016). Intention-aware motion planning using learning based human motion prediction. *CoRR*, abs/1608.04837.

Peternel, L. and Babic, J. (2013). Learning of compliant

human-robot interaction using full-body haptic interface. *Advanced Robotics*, 27:1003–1012.

Peternel, L., Tsagarakis, N., Caldwell, D., and Ajoudani, A. (2016). Adaptation of robot physical behaviour to human fatigue in human-robot co-manipulation. *IEEE-RAS International Conference on Humanoid Robots*, pages 489–494.

Siciliano, B. and Villani, L. (2000). *Robot Force Control*. Kluwer Academic Publishers, Norwell, MA, USA, 1st edition.